

# From Explicit Rules to Implicit Reasoning in an Interpretable Violence Monitoring System

Wen-Dong Jiang, *Graduate student Member, IEEE*, Chih-Yung Chang, *Member, IEEE*, Ssu-Chi Kuai, and Diptendu Sinha Roy, *Senior Member, IEEE*

**Abstract**— Recently, research based on pre-trained models has demonstrated outstanding performance in violence surveillance tasks. However, most of them were black-box systems which faced challenges regarding explainability during training and inference processes. An important question is how to incorporate explicit knowledge into these implicit models, thereby designing expert-driven and interpretable violence surveillance systems. This paper proposes a new paradigm for weakly supervised violence monitoring (WSVM) called Rule base Violence Monitoring (RuleVM). The proposed RuleVM uses a dual-branch structure with different designs for images and text. One of the branches is called the implicit branch, which uses only visual features for coarse-grained binary classification. In this branch, image feature extraction is divided into two channels: one responsible for extracting scene frames and the other focusing on extracting actions. The other branch is called the explicit branch, which utilizes language-image alignment to perform fine-grained classification. For the language channel design in the explicit branch, the proposed RuleVM uses the state-of-the-art YOLO-World model to detect objects in video frames, and association rules are identified through data mining methods as descriptions of the video. Leveraging the dual-branch architecture, RuleVM achieves interpretable coarse-grained and fine-grained violence surveillance. Extensive experiments were conducted on two commonly used benchmarks, and the results show that RuleVM achieved the best performance in both coarse-grained and fine-grained monitoring, significantly outperforming existing state-of-the-art methods. Moreover, interpretability experiments uncovered some interesting rules, such as the observation that as the number of people increases, the risk level of violent behavior also rises.

**Index Terms** —*Explanation, Interpretable Decision, Smart City, Violence Monitoring.*

This work was supported by the National Science and Technology Council of Taiwan, Republic of China, under grant number NSTC 112-2622-E-032-005. (Corresponding author: Chih-Yung Chang.)

Wen-Dong Jiang is currently pursuing a Ph.D. degree with the Department of Computer Science and Information Engineering, Tamkang University, New Taipei 25137, Taiwan. (e-mail: 812414018@o365.tku.edu.tw).

Chih-Yung Chang is with the Department of Computer Science and Information Engineering, Tamkang University, New Taipei 25137, Taiwan. (email: cychang@mail.tku.edu.tw).

Ssu-Chi Kuai is with the Department of Information Management, National Taipei University of Business, Taipei 100025, Taiwan. (email: sckuai@ntub.edu.tw).

Diptendu Sinha Roy is with the Department of Computer Science and Engineering, National Institute of Technology, Shillong, 793003, India (e-mail: diptendu.sr@nitm.ac.in).

## I. INTRODUCTION

THE primary goal of violent surveillance is to monitor abnormal events in the real world to prevent violent behavior and maintain social order [1]. With the rapid advancement of artificial intelligence, researchers are exploring the use of deep learning technologies in surveillance systems



Fig. 1. Interpretability Issues in Violence Surveillance Systems.

to replace the inefficiencies and high costs associated with traditional manual monitoring [2][3]. Weakly-supervised violence surveillance (WSVM) has emerged as an important research area in recent years. Unlike traditional methods, which require labeling every frame of a video and using supervised learning for frame-level training, WSVM achieves frame-level anomaly monitoring based on video-level annotations [4][5]. In current approaches, pre-trained models such as Inflated 3D ConvNet (I3D) [6], Transformer [7], and Contrastive Language-Image Pretraining (CLIP) [8] are often used to extract features from full-resolution frames. These features are subsequently processed using temporal sequence models, and finally, a Multiple Instance Learning (MIL) mechanism is applied to train classifiers for predicting anomalies at the frame level [9][10][11]. Although these methods have demonstrated strong performance, the increasing complexity of systems has raised growing concerns about interpretability [12]-[16].

Figure 1 highlights some of the interpretability issues found in benchmark datasets of current violence surveillance systems. As shown in Fig. 1, while the model successfully monitors the presence of violence in certain scenes, the interpretability machine learning method [13] reveals that the system made errors in its decision-making. It incorrectly identifies certain elements, such as scenes, colors, or even non-violent bystanders, as being associated with violence. This poses significant risks when applied in real-world contexts.

From a system design perspective, the root cause of this issue lies in the tendency of researchers to employ tightly coupled training processes rather than decoupled representation training. They often package the scene and abnormal behavior together as a fixed input to the system. This approach makes it difficult for the system to distinguish whether it should focus on behavior changes or scene changes during the temporal

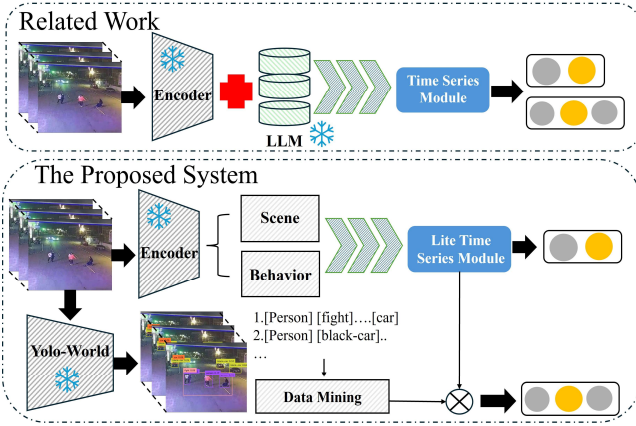


Fig. 2. Differences from previous studies

sequence and classifier training phases. As a result, the system may produce correct predictions but with flawed decision logic when operating in real-world scenarios.

Additionally, in many existing applications, traditional CCTV cameras typically rely solely on visual data, making it difficult to monitor certain potential violent events that cannot be captured through visual information alone. For instance, when someone holds up a sign or sends messages containing threatening content, it is challenging to discern intent or threats purely from video footage. These text-based signals might reveal signs of potential violence or dangerous behavior.

Recently, studies using pre-trained models that incorporate both image and text modalities, such as CLIP [17][18], have demonstrated excellent performance in violence surveillance tasks. The core idea of CLIP [8] is to align images and text through contrastive learning by pairing images with corresponding textual descriptions while excluding mismatched pairs in a shared embedding space. This alignment is achieved by calculating the distance between image and text embeddings: a smaller distance indicates a strong association, whereas a larger distance suggests that the two are unrelated.

Even in scenarios where only visual modality is available, and no additional modality sensors are present to capture other types of data, surveillance systems can still leverage these pre-trained models to perform multimodal training. This helps address problems that a single visual modality alone might not be able to resolve.

To address these issues, this paper proposes a violence surveillance system called RuleVM, specifically designed for WSVM. As shown in Fig. 2, unlike previous studies that directly adopt end-to-end coupled designs, the proposed RuleVM employs a differentiated, decoupled design for both image and text modalities and introduces a dual-branch structure to implement an end-to-end violence monitoring system.

In this paper, the proposed RuleVM is a two-branch system. The first branch, called the implicit branch, focuses on coarse-grained binary classification using visual features. In this branch, image feature extraction is divided into two channels: one for extracting scene frames and the other specifically for behavior extraction. The second branch, known as the explicit branch, performs fine-grained classification by leveraging the alignment between text and images. For the text

channel in the explicit branch, the proposed RuleVM integrates the state-of-the-art YOLO-World [20] to detect objects in video frames and apply data mining techniques to identify association rules, which provide interpretable, rule-based descriptions of the video content. Additionally, RuleVM incorporates a lightweight time series module to enable system deployment in edge computing scenarios.

With the advantages of dual-branch architecture, the proposed RuleVM achieves both coarse-grained and fine-grained interpretable violence surveillance. Extensive experiments conducted on the XD-Violence [21] and UCF-Crime [6] dataset demonstrate the superiority of the proposed method. In practice, this paper aims to solve the following three research challenges:

1. How can training data be effectively guided to the designed branches, ensuring the system collaborates to achieve both coarse-grained and fine-grained monitoring of violent behavior?
2. How can the system's computational efficiency be optimized without compromising accuracy in the explicit branch that uses YOLO-World and data mining techniques to extract association rules?
3. How can data patterns be extracted from training results to facilitate model optimization and uncover potential underlying trends?

In real-world applications, such as in large-scale sports events where thousands of spectators gather in stadiums, the environment is often filled with excitement and tension, which greatly increases the likelihood of conflicts or violent incidents. Traditional surveillance systems often rely solely on video footage to monitor abnormal behavior, making it difficult to accurately distinguish between potential violent acts and normal intense interactions within the crowd. This limitation can result in real threats being overlooked or false alarms being triggered. In summary, the contributions of this paper are as follows:

1. The proposed RuleVM employs dual-branch architecture, consisting of implicit and explicit branches. It decouples the originally integrated surveillance tasks into two parts responsible for coarse-grained and fine-grained monitoring of violent behavior. The implicit branch performs classification based solely on visual features, enabling the understanding of potential behaviors and the surrounding environment in the images. The explicit branch aligns text with video, utilizing rules and video to perform more detailed comparisons and classifications, making the model's decision-making process more transparent and easier to understand.
2. In the explicit branch, the proposed RuleVM uses the YOLO-World to detect objects in video and applies data mining techniques to mine association rules for video content descriptions. These descriptions provide natural language-level supplementary explanations for surveillance outcomes, enabling the model to explain its classification decisions in a readable manner, further improving the system's interpretability.
3. Extensive experiments conducted on benchmark datasets show that the proposed RuleVM has a

TABLE I  
COMPARISON WITH OTHER WORK

Related Works	Model	Fine-Grained and Coarse-Grained	Interpretable	Cross-modal	Real-Time	Accurate Prompt
[22] (2016)	C3D	Coarse-Grained	×	×	✓	×
[6] (2018)	I3D	Fine-Grained	×	×	✓	×
[25] (2021)	RTFM	Coarse-Grained	×	✓	×	×
[23] (2022)	OCSVM	Coarse-Grained	×	×	✓	×
[26] (2022)	AVVD	Fine-Grained and Coarse-Grained	×	×	×	×
[8] (2022)	CLIP	Coarse-Grained	×	✓	×	×
[4] (2023)	HL-Net	Fine-Grained and Coarse-Grained	×	×	×	×
[31] (2023)	UMIL	Coarse-Grained	×	✓	×	×
[32] (2023)	CLIP-TSA	Coarse-Grained	×	✓	×	×
[18] (2024)	VadCLIP	Fine-Grained and Coarse-Grained	×	✓	×	×
[17] (2024)	STPrompt	Fine-Grained and Coarse-Grained	×	✓	✓	×
Ours	RuleVM	Fine-Grained and Coarse-Grained	✓	✓	✓	✓

significant advantage over state-of-the-art competing methods. What is even more noteworthy is that, unlike other methods that only make predictions, RuleVM can output interpretable paths that clearly explain the reasons behind the model’s decisions, distinguishing it from other approaches.

The remainder of the paper is organized as follows. Section II discusses and compares previous relevant studies. Section III describes the assumptions and problem formulation in detail. Section IV details the proposed interpretable multimodal model. Section V provides experiments and performance evaluation. The conclusions are discussed in Section VI.

## II. RELATED WORK

This chapter presents a review of some relevant studies in Violence Monitoring. These studies are categorized into two parts: Weakly Supervised Violence Monitoring and Visual Language Pre-Training Models.

### A. Weakly Supervised Violence Monitoring

*Sultani et al.* [6] and *Hasan et al.* [22] were the first to introduce the MIL model for violence monitoring in supervised violence surveillance (SVM). The proposed approaches packaged surveillance videos into a package and then input them into I3D and C3D networks for binary classification of violent and non-violent events. *Ji and Lee* [23] proposed the One-Class Support Vector Machine (OCSVM) model for violence monitoring. However, due to the limitations of 3D network-based designs in terms of real-time performance and hardware requirements in practical applications, research gradually shifted towards combining video frame extraction and time series modules for violence monitoring. Subsequent research began to focus on using self-attention mechanisms, Transformer, or Graph ConvNet (GCN) to capture temporal and contextual relationships in video content. *Zhong et al.* [24] proposed a GCN-based method to calculate feature similarity and temporal consistency between monitored video segments for the monitoring of violent behavior. While *Tian et al.* [25] utilized a self-attention network to capture the global temporal context of violent behavior in monitoring videos. Their proposed model, referred to as Robust Temporal Feature

Magnitude (RTFM), effectively leverages temporal information to enhance the monitor of violent actions. *Wu et al.* [4] proposed Hierarchical Learning Network (HL-NET), which developed a global and local attention module to identify temporal dependencies and thereby obtain more expressive embeddings from monitoring videos.

All the above methods are based on an end-to-end coupled system design, which monitors abnormal events by predicting the probability of abnormal frames. However, this approach, which compresses each frame into a package and then inputs it into the time series module for an end-to-end MIL system, presents significant interpretability issues. Additionally, in the design of the time series module, these systems only consider application scenarios in a unified cloud environment and do not consider lightweight requirements in some edge computing scenarios.

### B. Visual language pre-training Models

In some practical application scenarios, only single-modal cameras were typically available, and traditional multi-modal designs were often not applicable to these single-modal scenarios. Thanks to certain pre-trained models, such as CLIP [8], which aligned text and images to accomplish multi-modal tasks, it became possible to achieve multi-modal tasks even in scenarios where only a single modality was present. For instance, *Zhou et al.* [26] introduced an enhanced image classification approach leveraging the CLIP, which significantly improved performance in complex visual recognition tasks. *Mokady et al.* [27] made a major advancement in automatic image captioning by refining the integration of vision and language models. *Zhou et al.* [28] applied CLIP to object monitoring, improving the model’s ability to distinguish between similar objects. *Yu et al.* [29] made notable progress in scene text monitoring, particularly in enhancing the accuracy and efficiency of text localization in cluttered environments. Additionally, *Rao et al.* [30] conducted valuable research on dense prediction tasks, focusing on improving the precision of pixel-level predictions in dense visual data. *Lv et al.* [31] proposed Uncertainty-aware Multiple Instance Learning (UMIL), which incorporated uncertainty estimation into the multiple instances learning framework to improve the system’s robustness and accuracy. *Joo et al.* [32] proposed CLIP with Temporal Shift Attention (CLIP-Tsa),

which introduces a temporal shift attention mechanism to better capture temporal dependencies in video data, enhancing the model's performance in tasks. In Violence Monitor, *Luo et al.* [33] proposed CLIP4Clip, a method aimed at transferring the knowledge of CLIP models to the field of video-text retrieval; *Wu et al.* [18] proposed Video Anomaly Monitor CLIP (VadCLIP), a simple yet powerful baseline that efficiently adapts pre-trained image-based visual-language models to leverage their robust capabilities in general video understanding. *Wu et al.* [17] introduced Spatio-Temporal Prompting (STPrompt), a CLIP-based three-branch architecture to address classification and localization in violence monitoring.

Although CLIP-based pre-trained models had achieved high performance in image-text matching tasks, their design typically focused more on the image branch, while the text branch relied on large language models (LLMs) to generate tokens, which were then transformed into embeddings through an encoder. In video tasks, the challenges for CLIP were particularly evident. Descriptions of videos were often represented in high-dimensional embeddings, which were too abstract, and even if tokens were generated, these tokens could not easily form understandable natural language descriptions. Instead, they often represented highly compressed information. Additionally, the output of LLMs could be inconsistent and unstable in some scenarios, further impacting the accuracy of the text branch.

Table I summarizes the aforementioned methods and compares them with the proposed model in terms of Fine-Grained and Coarse-grained, Interpretable, Cross-modal, Real-Time, and Accurate Prompt.

### III. ASSUMPTIONS AND PROBLEM FORMULATION

This section introduces the assumptions and problem statements of this study. Given a monitoring video sequence  $\mathcal{V}$  of duration  $t$ , partitioned into  $N$  equal-length temporal segments. The primary objective of this research is to ascertain the presence of anomalies within  $\mathcal{V}$ .

Let  $\mathcal{V} = \{\Phi_i\}_{i=1}^N$  denote the video sequence, where each segment  $\Phi_i$  may consist of non-violent content, violent content, or a combination thereof. Let  $\hat{\mathcal{V}}_i$  and  $\mathcal{V}_i$  denote the non-violent and violent subsets of  $\Phi_i$ , respectively. Each segment is defined as the union of its nonviolent and violent components  $\Phi_i = \hat{\mathcal{V}}_i \cup \mathcal{V}_i$ .

Let  $\mathcal{C} = \{c_\kappa\}_{\kappa=1}^{\mathcal{K}} \cup \{\hat{c}\}$  denote the set of all possible classes, where  $c_\kappa$  denotes the  $\kappa$ -th violence classes for  $1 \leq \kappa \leq \mathcal{K}$ , and  $\hat{c}$  denotes the non-violence class. Correspondingly, let  $L = \{\ell_\kappa\}_{\kappa=1}^{\mathcal{K}} \cup \{\hat{\ell}\}$  be the set of labels, where  $\ell_\kappa$  is the label associated with class  $c_\kappa$ , and  $\hat{\ell}$  is the label for the non-violence class  $\hat{c}$ , and  $\hat{l}$  is the label for the non-violence class  $\hat{c}$ .

This paper assumes that each  $\mathcal{V}_i$  of segment  $\Phi_i$  belongs to a specific violence class  $c_\kappa$  for  $\kappa \in \{1, 2, \dots, \mathcal{K}\}$ . Consider violence monitoring mechanism  $\mathcal{M} \in \mathfrak{M}$ , where  $\mathfrak{M}$  denotes the space of all admissible monitoring mechanisms. The mechanism  $\mathcal{M}$  aims to monitor the occurrence of violent events within  $\mathcal{V}$ .

For each segment  $\Phi_i$ , mechanism  $\mathcal{M}$  assigns a confidence score  $\mathcal{P}_i \in [0, 1]$ , indicating the likelihood that  $\Phi_i$  contains

violence. Let  $\theta \in [0, 1]$  denote a predetermined prediction threshold. Define the prediction indicator  $\delta_i^{\mathcal{M}}(\theta)$  for segment  $\Phi_i$  represent in  $\delta_i^{\mathcal{M}}(\theta) = \begin{cases} 1, & \text{if } \mathcal{P}_i \geq \theta; \\ 0, & \text{if } \mathcal{P}_i < \theta. \end{cases}$  Define the ground truth indicator  $\delta_i$  for segment  $\Phi_i$  as  $\delta_i = \begin{cases} 1, & \text{if } \mathcal{V}_i \neq \emptyset; \\ 0, & \text{if } \mathcal{V}_i = \emptyset. \end{cases}$

Let  $TP_i, TN_i, FP_i$  and  $FN_i$  represent True Positive, True Negative, False Negative and False Positive respectively, of the prediction result of input  $\hat{\mathcal{V}}_i$  by applying mechanism  $\mathcal{M}$ . The values can be calculated using  $TP_i = \delta_i \times \delta_i^{\mathcal{M}}(\theta)$ ,  $TN_i = (1 - \delta_i) \times (1 - \delta_i^{\mathcal{M}}(\theta))$ ,  $FP_i = (1 - \delta_i) \times (1 - \delta_i^{\mathcal{M}}(\theta))$  and  $FN_i = \delta_i \times (1 - \delta_i^{\mathcal{M}}(\theta))$ , respectively.

Let  $TP, TN, FP$  and  $FN$  represent the cumulative True Positive, True Negative, False Positive, and False Negative, respectively, of the prediction results by applying mechanism  $\mathcal{M}$  to all segments  $\Phi_i$ , for  $1 \leq i \leq N$ . The value can be calculated by  $TP = \sum_{i=1}^N TP_i$ ,  $TN = \sum_{i=1}^N TN_i$ ,  $FP = \sum_{i=1}^N FP_i$  and  $FN = \sum_{i=1}^N FN_i$ , respectively.

Let  $\mathcal{P}^{\mathcal{M}}, \mathcal{R}^{\mathcal{M}}$  denote the Precision and Recall of the predictions by applying mechanism  $\mathcal{M}$  to predict a given video  $\mathcal{V}$ . The values of  $\mathcal{P}^{\mathcal{M}}, \mathcal{R}^{\mathcal{M}}$  can be calculated by  $\mathcal{P}^{\mathcal{M}} = \frac{TP}{TP+FP}$  and  $\mathcal{R}^{\mathcal{M}} = \frac{TP}{TP+FN}$ , respectively.

Let  $\theta_j$  denote the  $j$ -th prediction threshold, let  $\mathcal{AP}^{\mathcal{M}}$  denote the *Average Precision* of mechanism  $\mathcal{M}$ . The  $\mathcal{AP}^{\mathcal{M}}$  can be calculated by **Exp. (1)** :

$$\mathcal{AP}^{\mathcal{M}} = \sum_{\kappa=1}^{K-1} (\mathcal{R}^{\mathcal{M}}(\theta_{\kappa+1}) - \mathcal{R}^{\mathcal{M}}(\theta_\kappa)) \times \mathcal{P}(\theta_{\kappa+1})^{\mathcal{M}}.$$

Similar to previous works [4], [8], [17], [18] the first objective of this paper is to develop mechanism  $\mathcal{M}^{best}$  that satisfies  $\mathcal{M}^{best} = \arg \max_{\mathcal{M} \in \mathfrak{M}} (\mathcal{AP}^{\mathcal{M}})$ .

Let  $\mathcal{A}_{\mathcal{M}}$  denote the *AUC* of mechanism  $\mathcal{M}$ . The value of  $\mathcal{A}_{\mathcal{M}}$  can be calculated by **Exp. (2)**:

$$\mathcal{A}_{\mathcal{M}} = \int_0^1 TPR(\theta) d(FPR(\theta)) = \int_0^1 \frac{TP(\theta)}{TP(\theta) + FN(\theta)} d\left(\frac{FP(\theta)}{FP(\theta) + TN(\theta)}\right).$$

Similar to previous works [4], [8], [17], [18] the second objective of this paper is to develop mechanism  $\mathcal{M}^{best}$  that satisfies  $\mathcal{M}^{best} = \arg \max_{\mathcal{M} \in \mathfrak{M}} (\mathcal{A}_{\mathcal{M}})$ . This section introduced the assumptions and problem formulation of this paper. The next section will introduce the proposed RuleVM.

### IV. THE PROPOSED RULEVM

This section presents the proposed RuleVM system which aims to develop an interpretable violence monitoring system. Unlike previous works [4][26][31][32], which designed a coupled end-to-end black-box system by integrating multiple pre-trained models, the proposed RuleVM adopts a decoupling design strategy, designs implicit and explicit branches and employs a multi-channel approach for achieving an interpretable violence monitoring system. This allows each branch to handle its respective task independently during the training process without interference from other noise.

Furthermore, regarding the design of the textual branch, in contrast to previous works [17][18][31][32], which directly

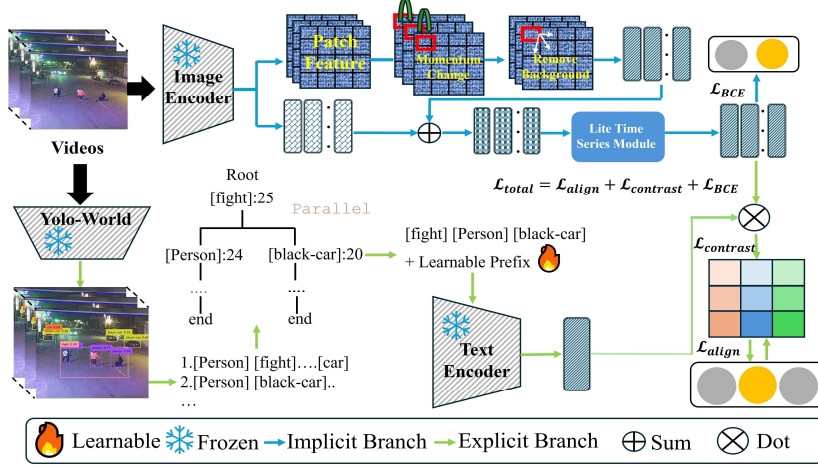


Fig. 3. The pipeline of the proposed RuleVM system

used LLMs to generate descriptions for each frame and then obtained video embedding through a temporal module, the proposed RuleVM combines a pre-trained object detection model with data mining techniques to derive the rules for video descriptions. This enables RuleVM to maintain strong interpretability, during both training and deployment phases. Finally, compared to previous works [4][6][17][18][22][25], the proposed RuleVM uses a lightweight temporal module, allowing the model to consume significantly fewer computational resources in both training and deployment phases compared to other systems.

Figure 3 illustrates the detailed architecture of the proposed RuleVM system. The system consists of two branches: the Implicit Branch and the Explicit Branch. Each branch has two respective channels. The Implicit Branch utilizes visual features and a lightweight temporal sequence module to perform coarse-grained binary classification. It is designed to jointly extract spatial information at the frame level through both the behavior and scene channels, then analyze the temporal relationships using the lightweight temporal module, and finally train the branch through a binary classifier. Then the explicit Branch achieves fine-grained multi-class classification using both text and images, with its two channels corresponding to text and video, respectively. The text is derived from YOLO-World and association rules generated by data mining methods, while the video is represented by the embedding produced by the Implicit Branch before executing binary classification. The text and video embeddings are combined through contrastive learning in high-dimensional space to generate a consistent embedded state, which is then used for branch training in multi-class classification. The following provides further details:

#### A. Implicit Branch

The goal of the Implicit Branch is to capture potential implicit representations in surveillance videos through the processing of visual features. This branch is divided into three parts: feature extraction of the scene channel, feature extraction of the behavior channel, and lite time-series module.

##### 1. Scene Channel

The purpose of designing scene channels is to obtain the representation of each frame in the video. Let  $V = \{f_1, f_2, \dots, f_n\}$  denote the video sequence consisting of  $n$  frames, where each frame  $f_j \in \mathcal{F}$  for  $j \in \{1, 2, \dots, n\}$ . Each frame is processed using a frozen CLIP Image Encoder to extract frame-level features. Let  $\mathcal{F}$  represent the space of frames and  $\mathcal{F}_{clip}$  represent the feature space derived by the CLIP Image Encoder. Define  $\Phi: \mathcal{F} \rightarrow \mathcal{F}_{clip}$  as the feature extraction function implemented by the CLIP Image Encoder. Therefore, the frame-level feature representations are given by:

$$V_{clip} = \{\Phi(f_1), \Phi(f_2), \dots, \Phi(f_n)\} = \{g_1^{scene}, g_2^{scene}, \dots, g_n^{scene}\},$$

where  $g_j^{scene} = \Phi(g_j) \in \mathcal{F}_{clip}$  denotes the scene channel feature extracted from the  $j$ -th frame by frozen CLIP Image Encoder. After the scene channel feature extraction, Next is behavior channels.

##### 2. Behavior Channel

The purpose of designing behavior channels is to capture changes between frames content to guide the model in identifying action changes within a scene. Previous studies typically utilized optical flow methods [34][35] to monitor action change. However, these methods have two main issues: first, optical flow may not be accurate in some violent scenes occurring at dusk. Second, the computational cost of optical flow is relatively high. To address this problem, an Efficient Behavior Monitoring Module (EBMM) is proposed to achieve fast and effective action change monitoring.

The proposed EBMM operates a two-stage monitoring mechanism. In the first stage, it captures motion changes by computing differences between consecutive frames. In the second stage, it removes background information by calculating changes between neighboring patches within the current frame.

Let  $p_i^k$  denote the  $k$ -th patch in the  $i$ -th frame, for a subset of the feature maps  $V_{clip} = \{g_1^{scene}, g_2^{scene}, \dots, g_n^{scene}\}$ . The proposed EBMM divides each frame into  $m$  patches, resulting in a corresponding patch set  $P_i = \{p_i^1, p_i^2, \dots, p_i^m\}$ . In the first stage, the proposed EBMM computes the motion difference for

each patch by calculating the change between consecutive frames:  $\Delta p_i^k = p_i^k - p_{i-1}^k$ , where  $i = 2, \dots, n$  and  $k = 1, \dots, m$ .

In the second stage, the proposed EBMM removes background effects. Let  $N(k)$  denote the neighboring patch which consists of patches adjacent to  $p_i^k$ . For each neighboring patch  $p_i^l$  where  $l \in N(k)$ , calculate the absolute difference in That is,  $\delta p_i^{k,l} = |p_i^k - p_i^l|$ . To obtain the background suppression value and aggregation. That is:

$$\delta p_i^k = p_i^k - \frac{1}{|N(k)|} \sum_{l \in N(k)} p_i^l, \quad (3)$$

the total difference for each patch is then given by

$$S_i^k = |\Delta p_i^k| + |\delta p_i^k|.$$

Let  $A_i$  denote the weight scores computed by applying an exponential kernel function over the total differences  $S_i^k$ . The calculation of  $A_i$  as shown in **Exp. (4)**:

$$A_i = \frac{e^{\alpha S_i^k}}{\sum_j e^{\alpha S_j^k}}, \quad (4)$$

Herein, the  $\alpha$  denotes the Hyperparameters. The weight scores are expanded to match the original patch structure. These expanded scores are then used to adjust the total difference scores  $S_i^k$  for all patches in the frame. Let  $S_i^{Behavior}$  denote the final representation, the calculated as shown in **Exp. (5)**:

$$S_i^{Behavior} = A_i^T \cdot S_i^k \quad (5)$$

According to Exp. (4), the  $S_i^{Behavior}$  can receive higher weights, while background patches are weighed close to zero. Unlike  $g_j^{scene}$ , where all pixels in each frame have nearly equal influence in violent surveillance scenes,  $S_i^{Behavior}$  places a strong emphasis on locations of violent behavior. Since the relationship between  $S_i^{Behavior}$  and  $g_j^{scene}$  is complementary, they are added together and fed into a lightweight temporal sequence module for further processing.

### 3. Lite time-series module

Till now, the proposed scene channel and behavior channel extract frame-level background and action features using the CLIP encoder. These features contain instantaneous information but lack the global temporal context crucial for WSVM tasks. In this section, a lightweight temporal sequence module is proposed, which is similar to the standard Receptance Weighted Key Value (RWKV) [36] encoder, including self-attention, layer normalization (LN), and feed-forward network (FFN). Since the positions of frames in sequence data are already fixed, there is no need to apply positional encoding when training the temporal sequence module. The main difference between this approach and traditional RWKV or other Transformer-like encoders lies in the computation of self-attention, which is based on relative distance rather than feature similarity. This mechanism makes the model more lightweight, as it effectively reduces the complexity of attention computation by considering only the relative distance between frames, without the need to evaluate high-dimensional feature

similarity. This helps reduce computational costs and makes training and inference more efficient.

Specifically, in the design of self-attention, let  $\kappa$  denote adjacency matrix. Since the similarity between  $i$ -th and  $j$ -th frames is only determined by their relative temporal distance, the value of  $\kappa$  is calculated as  $\kappa = \frac{-|i-j|}{\sigma}$ , where  $\sigma$  is a hyperparameter to control the range of influence of distance relation. In this work, the input of *Lite time-series module* is the summation feature of  $f_j^{scene}$  and  $S_i^{Behavior}$ .

The operation of the time series module can be treated as a two-stage process. In the first stage, the time series model utilizes the attention mechanism of  $\kappa$ , computed through *Softmax* and *Layer Normalization* (LN), to incorporate temporal information into the features, thereby analyzing the input time series. Let  $\Psi$  denote the feature with temporal information fused after the first step. The operation of the first stage is represented as shown in **Exp. (6)**:

$$\Psi = \text{LN}(\text{Softmax}(\kappa)(S_i^{Behavior} + f_j^{scene})), \quad (6)$$

In the second stage,  $\Psi$  is processed through a *Feed-Forward Network* (FFN), followed by a residual connection, and then through Layer Normalization to obtain the result. Let  $\psi$  denote the output after the non-linear transformation and residual connection in the second step. The operation of the second stage is represented as shown in **Exp. (7)**:

$$\psi = \text{LN}(\text{FFN}(\Psi) + \Psi). \quad (7)$$

After completing the time series processing, in the Implicit Branch, a coarse-grained binary classifier is integrated. The classification objective function is adopted for the classification branch, which is presented as shown in **Exp. (8)**:

$$\mathcal{L}_{BCE} = -\frac{1}{N} \sum_{i=1}^N [y_i \log(\hat{y}_i) + (1 - y_i) \log(1 - \hat{y}_i)], \quad (8)$$

where  $\mathcal{L}_{BCE}$  represents the cross-entropy loss,  $N$  is the number of samples,  $y_i$  is the true label of the  $i$ -th sample and  $\hat{y}_i$  is the predicted probability for the  $i$ -th sample. The above provides the complete content of the implicit branch; next, the explicit branch will be introduced.

#### (B). Explicit Branch

The goal of the explicit branch is to perform fine-grained multi-class classification by utilizing contrastive learning between text and video. This branch is divided into two parts: rule generation based on YOLO-World and data mining, and contrastive learning between text and video.

##### 1. Rule Generation

The purpose of rule generation is to create more interpretable video descriptions. Previous studies [17][18][31][32] typically used LLMs to generate descriptions for each frame, followed by temporal sequence models to obtain a textual embedding representation for the entire video. However, these methods have two main issues. First, the embedding representation is usually high-dimensional and lacks interpretability. Second, the LLMs tend to be unstable, making it difficult to ensure consistent scene descriptions for

each frame. To address these problems, this paper employs a two-stage approach that combines object monitor and data mining to generate interpretable video descriptions. The following are the specific details:

Firstly, object detection is considered. In practice, the pre-trained model YOLO-World [20] is used to monitor the actions and objects presented in each frame. YOLO-World is a model pre-trained on a large-scale dataset through vision-language modeling, capable of efficient zero-shot detection. Specifically, given an image  $I$  and a set of categories  $U = \{U_1, U_2, \dots, U_j\}$  that need to be monitored, the model can automatically identify and outline the corresponding objects in the image  $I$ . For a video  $V = \{f_1, f_2, \dots, f_n\}$ , the model monitors each frame, resulting in  $n$  pieces of data containing the objects monitored in each frame and their corresponding counts.

The goal of data mining here is to derive association rules from the given data. For instance, by using YOLO-World to analyze a video of a fight, it is possible to extract the ongoing actions and objects involved. By calculating the confidence and support of the objects appearing in each frame, the rule:

$$\{\text{People}\}\{\text{Strick}\} \rightarrow \{\text{Fight}\},$$

can ultimately be derived. This means that whenever people and sticks are present, it is likely that a fight is occurring. By referring the FP-Growth [37], this paper further improves efficiency in terms of the required time for data mining. Specifically, FP-Growth is a two-phase process involving the construction and pruning of an FP-Tree. Data mining is conducted through conditional judgments, tree structures, and frequency counting. However, using GPUs does not significantly enhance the efficiency of these operations, as they primarily rely on logical operations and conditional evaluations rather than parallel matrix computations. On the other hand, traditional CPUs experience efficiency degradation due to I/O constraints [38].

To address these issues, this paper proposes a multi-CPU parallel FP-Growth method. In this approach, data are divided into separate blocks and are processed in parallel across different CPU threads to construct multiple FP-Trees, which are eventually merged into a complete tree for data mining. The following defines the notations that will be used to present the proposed MCP-FP Algorithm. The detailed operations are given in the MCP-FP Algorithm.

## 2. Contrastive Learning

In violent behavior monitoring tasks, traditional single-modal information often has limitations in recognizing specific violent behaviors. Therefore, this paper explores multi-modal information to improve recognition performance. Cross-modal learning is a powerful approach because it can integrate data from different sources, such as visual and textual information, providing richer semantic understanding and stronger recognition capabilities.

This paper introduces the method of contrastive learning which aims to enhance the model's recognition ability by maintaining consistency across different modalities. Here, CLIP is a typical cross-modal contrastive learning model, which consists of two encoders: an image encoder and a text

### Definitions:

Notations	Meaning
$D$	Dataset
$\{D_1, D_2, \dots, D_n\}$	Non-overlapping data blocks, where $D = \bigcup_{i=1}^n D_i$ and $D_i \cap D_j = \emptyset$ for $i \neq j$ .
$\text{min\_support} \in [0,1]$	Minimum support threshold.
$\text{min\_confidence} \in [0,1]$	Minimum confidence threshold.
$\text{freq}_i(x)$	Frequency (count) of item
$\text{support}(x) = \sum_{i=1}^n \text{freq}_i(x)$	support of item $x$ in the entire dataset $D$ .
$L_i$	local frequent itemset for $D_i$ , where $L_i = \{x   x \in D_i, \text{freq}_i(x) \geq \text{min\_support}\}$ .
$\text{FP\_Tree}_i$	FP-trees were constructed from $L_i$ and $D_i$ .
$\text{FP\_Tree}_{\text{global}}$	Global FP-tree constructed by merging all $\text{FP\_Tree}_i$ .
$F$	Set of global frequent itemset $\text{min\_support}$
$R$	set of association rules satisfying $\text{min\_support}$ and $\text{min\_confidence}$ .

### MCP-FP Algorithm: Multi-CPU Parallel FP-Growth Construction

Input: Dataset  $D = \bigcup_{i=1}^n D_i$ , divided into multiple chunks  $\{D_1, D_2, \dots, D_n\}$ ,  $\text{min\_support} \in [0,1]$ , and  $\text{min\_confidence} \in [0,1]$ .

Output: Set of association rules  $R$ .

```

Initialize  $R \leftarrow \emptyset$  and  $F \leftarrow \emptyset$ 
For  $i = 1$  to  $n$  do:
  Assign  $D_i$  to CPU  $i$ .
  Parallel for  $i = 1$  to  $n$  do:
    For each item  $x \in D_i$ :
       $\text{freq}_i(x) \leftarrow$  count of  $x$  in  $D_i$ .
       $\text{support}(x) \leftarrow \text{support}(x) + \text{freq}_i(x)$ 
     $L_i \leftarrow \{x | \text{support}(x) \geq \text{min\_support} \times |D|\}$ 
     $\text{FP\_Tree}_i \leftarrow$  ConstructFPtree( $L_i, D_i$ )
    Initialize  $\text{FP\_Tree}_{\text{global}} \leftarrow$  empty  $\text{FP\_Tree}$ 
    For  $i = 1$  to  $n$  do:
      For each node  $x$  in  $\text{FP\_Tree}_i$ :
        If  $x$  exists in  $\text{FP\_Tree}_{\text{global}}$ :
           $\text{FP\_Tree}_{\text{global}}(x) \leftarrow \text{FP\_Tree}_{\text{global}}(x) + \text{FP\_Tree}_i(x)$ 
        else
          Add node  $x$  to  $\text{FP\_Tree}_{\text{global}}$  with count  $\text{FP\_Tree}_i(x)$ 
    Parallel for each FP-tree  $T_{\text{conditional}}$  derived from  $\text{FP\_Tree}_{\text{global}}$  do:
       $F \leftarrow F \cup \text{MineFrequentItemsets}(T_{\text{conditional}}, \text{min\_support})$ 
      For each frequent itemset  $f \in F$ :
        For each non-empty subset  $s \subset f$ :
           $\text{conf} \leftarrow \frac{\text{support}(f)}{\text{support}(s)}$ 
          If  $\text{conf} \geq \text{min\_confidence}$ :
             $R \leftarrow R \cup \{s \rightarrow f \setminus s\}$ 
Output  $R$ 

```

encoder. The main function of CLIP is to transform images and text into vectors and calculate their similarity, ensuring that the representations of related images and text are close to each other in the vector space. This enables the vectors of images and text to query each other, achieving full fusion of the vector representations in both image and text spaces, resulting in more comprehensive multi-modal recognition.

This paper uses both visual and textual information for recognition. One challenge is to effectively obtain enough textual information. Typically, cameras used for video recording do not support audio recording or audio-to-text conversion. The lack of sufficient textual descriptions can negatively impact the effectiveness of cross-modal learning. As a result, it is crucial to consider how to address this issue.

In the text branch, this paper designs two inputs. One input employs YOLO-World in combination with parallel FP-Growth to mine video descriptions, while the other is a learnable prompt used for dynamically adjusting the output to more accurately capture key features and content in the video. Let  $T^{Rule} = \{T_1^{Rule}, T_2^{Rule}, \dots, T_m^{Rule}\}$  denote the video descriptions. Let  $T^{Prompt} = \{T_1^{Prompt}, T_2^{Prompt}, \dots, T_m^{Prompt}\}$  denote the Learnable prompt. These two inputs are combined as the shared input for the CLIP text encoder, yielding  $\phi^{text} = \{\phi_1^{text}, \phi_2^{text}, \dots, \phi_m^{text}\}$ . For image branch an embedding representation is directly adopted, using the output from **Exp. 7** in **Section c** to obtain  $\psi^{video} = \{\psi_1^{video}, \psi_2^{video}, \dots, \psi_m^{video}\}$ . The alignment matrix  $M_{m \times m} = [s_{i,j}]$  consists of the similarities between  $m$  video features and  $m$  text features, as shown in the following **Exp. (9)** :

$$M_{m \times m} = \begin{matrix} & \psi_1^{video} & \dots & \psi_m^{video} \\ \begin{matrix} F_1^{text} \\ \vdots \\ F_m^{text} \end{matrix} & \begin{bmatrix} s_{1,1} & \dots & s_{1,m} \\ \vdots & \ddots & \vdots \\ s_{m,1} & \dots & s_{m,m} \end{bmatrix} \end{matrix} \quad (9)$$

The similar value of  $s_{i,j}$  in the  $i$ -th row and  $j$ -th column of matrix  $M$  can be calculated in  $p_{i,j} = \frac{\exp(s_{i,j}/\tau)}{\sum_j \exp(s_{i,j}/\tau)}$ , where  $\tau$  is a scaling hyper parameter. The loss function of the entire model includes the alignment loss  $\mathcal{L}_{align}$  and contrastive loss  $\mathcal{L}_{contrast}$ . The alignment loss  $\mathcal{L}_{align}$  is shown in **Exp. (10)**:

$$\mathcal{L}_{align} = - \sum_{i=1}^m y_i \log(p_i) + \lambda_1 \|\theta_{align}\|^2, \quad (10)$$

where  $y_i$  represents the labels,  $\lambda_1$  controls the regularization of the model parameters in the alignment loss, and  $\theta_{align}$  represents the model parameters related to the alignment loss.

The contrastive loss  $\mathcal{L}_{contrast}$  calculates the cosine similarity between normal class embeddings and other abnormal class embeddings, as shown in **Exp. (11)**:

$$\mathcal{L}_{contrast} = \sum_j \max \left( 0, \frac{t_n \cdot t_{aj}}{\|t_n\|_2 \cdot \|t_{aj}\|_2} - \delta \right) + \lambda_2 \|\theta_{contrast}\|^2,$$

where  $t_n$  represents the embeddings of the normal class,  $t_{aj}$  represents the embeddings of the abnormal class,  $\delta$  is a hyper parameter,  $\lambda_2$  is a regularization parameter, and  $\theta_{contrast}$  represents the model parameters related to the contrastive loss. The final total loss function is shown in **Exp. (12)**:

$$\mathcal{L}_{total} = \mathcal{L}_{align} + \mathcal{L}_{contrast} + \mathcal{L}_{BCE}. \quad (12)$$

Through this design, the implicit and explicit branches are used for collaborative training and are integrated into an end-to-end system, ensuring that each loss function plays a unique role in the optimization process, aiming to prevent overfitting. During model training, the CLIP encoders are frozen, and the model fine-tunes both branches through backpropagation.

The above describes the entirety of the proposed RuleVM system. In the next section, the experiments and model performance will be introduced.

## V. MODEL PERFORMANCE

In this section, relevant experimental performance and analysis are presented.

### A. Dataset and Evaluation Metrics

The experiments utilized two popular datasets from the WSVM domain: UCF-Crime [6] and XD-Violence [21]. XD-Violence, the largest publicly accessible dataset in violence monitoring, contains 4,754 videos amounting to 217 hours and spans six categories of violent incidents: verbal abuse, car accidents, explosions, fights, riots, and shootings. This dataset is randomly split into a training set with 3,954 videos and a test set with 800 videos, where the test set includes 500 violent and 300 non-violent videos. The UCF-Crime dataset comprises 1,900 real-world surveillance videos, with 1,610 videos designated for training and 290 for testing.

In terms of evaluation metrics, the experiment follows the setup described in **Chapter III**. Specifically, in the XD-Violence dataset, the evaluation metric  $\mathcal{AP}^M$  from **Exp. (1)** is used, while in the UCF-Crime dataset, the metric  $\mathcal{A}_M$  from **Exp. (2)** is applied. This configuration is consistent with previous studies [4][6][8][17][18][22][23][32].

### B. Implementation Details

In practice, this study follows previous studies [17][18][32] by using a frozen CLIP (ViT-B/16) to extract features from video frames. For the XD-Violence and UCF-Crime datasets, the experiment processes 1 out of 16 frames on UCF-Crime dataset. During the training stage, the maximum length of training videos is set to 256; videos exceeding this limit are sampled down to this length. For all datasets, the length of the learnable prompts prefixed to text labels is set to 8. For each image patch  $p_i$ , the image is resized to  $224 \times 224$ , and a sliding window of  $32 \times 32$  with a stride of 32 is used to generate multiple patches.

For hyperparameter settings,  $\alpha$  in **Exp. (3)** is uniformly set to 0.25. The  $\lambda_1$  in **Exp. (10)** is  $5 \times 10^{-4}$  for the XD-Violence dataset and  $1 \times 10^{-3}$  for the UCF-Crime dataset. The  $\lambda_2$  in **Exp. (11)** is  $6 \times 10^{-4}$  for the XD-Violence dataset and  $2 \times 10^{-3}$  for the UCF-Crime dataset. The  $\sigma$  in adjacency matrix  $\kappa$  is 0.8, the  $\tau$  in  $p_{i,j}$  is 0.19.

For model optimization, the AdamW optimizer with a learning rate of  $1e-4$  is used to train the model on an NVIDIA A100 SXM4, with a batch size set to 128. In the data mining practice, an Intel Core i7-10700K is utilized.

### C. Comparison with State-of-the-art Methods

The proposed RuleVM can simultaneously realize coarse-grained and fine-grained violence monitoring. The experiment presents the performance of the proposed RuleVM and compares it with several state-of-the-art methods on coarse-grained and fine-grained WSVM tasks.

Table II compares the performance of the proposed RuleVM with other approaches on the XD-Violence and UCF-Crime datasets for coarse-grained monitoring. The results show that the proposed RuleVM performs excellently on both datasets, significantly outperforming other semi-supervised and

TABLE III  
FINE-GRAINED COMPARISONS ON XD-VIOLENCE AND UCF-CRIME.

Method	Mean $\mathcal{AP}^M@IoU$ (%) (XD-VIOLENCE.)						Mean $\mathcal{AP}^M@IoU$ (%) (UCF-CRIME.)					
	0.1	0.2	0.3	0.4	0.5	AVG	0.1	0.2	0.3	0.4	0.5	AVG
Random Baseline	1.82	0.92	0.48	0.23	0.09	0.71	0.21	0.14	0.04	0.02	0.01	0.08
SVM	18.64	12.53	11.05	8.26	4.32	10.96	3.64	3.59	2.39	1.34	0.98	2.39
OCSVM [23]	19.85	9.06	8.56	6.55	6.03	10.01	4.85	4.44	2.33	1.85	1.56	3.01
C3D [22]	20.28	13.72	8.44	5.06	2.81	10.06	4.33	3.88	2.46	1.66	2.11	2.89
I3D [6]	22.72	15.57	9.98	6.20	6.78	12.25	5.73	4.41	2.69	1.93	1.44	3.24
HL-Net [4]	35.35	28.02	20.94	15.01	10.33	21.93	8.47	6.88	5.62	4.91	3.38	5.85
CLIP-TSA [32]	34.53	32.88	28.11	13.65	10.01	23.84	12.62	8.13	6.66	4.28	1.91	6.72
VadCLIP [18]	37.03	30.84	23.38	17.90	14.31	24.70	11.72	7.83	6.40	4.53	2.93	6.68
STPrompt [17]	39.58	31.26	<b>28.35</b>	19.28	<b>16.29</b>	26.95	12.59	<b>8.13</b>	6.67	<b>5.30</b>	<b>3.54</b>	7.25
<b>RuleVM (Ours)</b>	<b>41.29</b>	<b>38.88</b>	27.64	<b>21.33</b>	13.79	<b>28.59</b>	<b>18.82</b>	7.66	<b>7.16</b>	5.02	3.51	<b>8.43</b>

TABLE II  
COARSE-GRAINED COMPARISONS ON XD-VIOLENCE ( $\mathcal{AP}^M$ )  
AND UCF-CRIME ( $\mathcal{A}_M$ ).

Category	Method	$\mathcal{AP}^M$	$\mathcal{A}_M$
Semi supervised	SVM baseline	50.80	50.10
	OCSVM [23]	28.63	63.20
	C3D [22]	31.25	51.20
Weak supervised	CLIP [8]	76.57	84.72
	I3D [6]	75.18	84.14
	HL-Net [4]	80.00	84.57
	CLIP-TSA [32]	82.17	87.58
	VadCLIP [18]	84.51	88.02
	STPrompt [17]	85.22	88.08
	<b>RuleVM (Ours)</b>	<b>87.48</b>	<b>89.63</b>

classification-based weakly supervised methods. Overall, RuleVM achieves 87.48%  $\mathcal{AP}^M$ , on the XD-Violence dataset and 88.58%  $\mathcal{A}_M$  on the UCF-Crime dataset, reaching the current state-of-the-art results. Compared to its strongest competitors, VadCLIP and STPrompt, the proposed RuleVM improves the  $\mathcal{AP}^M$  metric on the XD-Violence dataset by 2.97% and 2.26%, respectively, and exceeds the  $\mathcal{A}_M$  metric on the UCF-Crime dataset by 1.61% and 1.55%, respectively.

This performance improvement is primarily attributed to the use of an implicit branch and multi-channel training strategy in the proposed RuleVM. This approach jointly extracts frame-level spatial information through behavior and scene channels. Then the proposed RuleVM employs a lightweight temporal module to analyze temporal relationships. The advantages of this design are that RuleVM effectively separates and processes behavior and scene feature, avoids information conflicts, and significantly enhances model interpretability. Additionally, the end-to-end training approach allows coarse-grained tasks to leverage the knowledge from fine-grained implicit branches, resulting in more pronounced effects in coarse-grained monitoring tasks. Regarding the performance of fine-grained WSVM tasks, Table III presents a comparison of the RuleVM system developed in this paper with other related studies, such as VadCLIP and STPrompt, on the XD-Violence and UCF-Crime datasets. For fairness, all feature extractors utilize CLIP (ViT-B/16). Compared to coarse-grained experiments, fine-grained tasks in WSVM are more challenging, as they require not only monitoring the occurrence of violent events but also

accurately identifying the specific categories of violent types.

As shown in Table III, the proposed RuleVM system outperforms other methods on the XD-Violence and UCF-Crime datasets. This advantage is primarily due to the input strategy employed in the RuleVM system’s text encoder. Unlike methods that directly use text generated by LLM, the proposed RuleVM system combines association rules generated through data mining with learnable prompts as input. This approach not only produces a highly condensed and interpretable video description but also enhances the system’s ability to identify violent events. Through this input strategy, the system focuses on task-relevant semantic space and captures subtle distinctions in events, resulting in greater accuracy and stability in fine-grained classification tasks.

### C. Ablation Studies

Table IV presents the ablation study on the three modules within the two branches of the proposed RuleVM system. As shown in Table IV, all three modules are essential across both benchmark datasets, XD-Violence and UCF-Crime. Compared with the related studies, when a single module is used, system performance improves, though the gains are limited compared to combining multiple modules. Notably, when the FP-Growth module is combined with either the EBMM or RWKV module, significant performance enhancements are observed, indicating that FP-Growth provides crucial information gain by mining association rules. When all three modules are applied simultaneously, the system achieves optimal performance, with high accuracy rates of 87.48%  $\mathcal{AP}^M$  value on XD-Violence and 89.63%  $\mathcal{A}_M$  value on UCF-Crime. These results show the importance of multi-module synergy for violence monitoring tasks.

TABLE IV  
EFFECTIVENESS OF EACH MODULE

Components			XD-VIOLENCE	UCF-CRIME
EBMM	RWKV	FP-Growth	$\mathcal{AP}^M$	$\mathcal{A}_M$
✓			62.11	60.88
	✓		63.34	58.65
		✓	68.85	42.33
✓	✓		72.44	69.88
✓		✓	76.85	74.26
	✓	✓	73.59	72.11
✓	✓	✓	<b>87.48</b>	<b>89.63</b>

Table V presents the ablation study on the designed EBMM module. As shown in Table V, the dual-channel design achieves significant performance improvements on both benchmark datasets. When using only the scene or behavior channel individually, system performance reaches 81.35 and 84.61  $\mathcal{AP}^M$  value on XD-Violence and 83.65 and 85.53  $\mathcal{A}_M$  value on UCF-Crime, respectively. However, when both the scene and behavior channels are activated simultaneously, the system achieves optimal performance. These results indicate that the scene and behavior channels capture complementary aspects of abnormal features, and their combination enables a more comprehensive improvement in violence monitoring.

TABLE V

ABLATION STUDIES ON EBMM MODULE

Components		XD-VIOLENCE	UCF-CRIME
Scene Channel	Behavior Channel	$\mathcal{AP}^M$	$\mathcal{A}_M$
✓		81.35	83.65
	✓	84.61	85.53
✓	✓	<b>87.48</b>	<b>89.63</b>

TABLE VI

ABLATION STUDIES ON TIME SERIES MODULE

Method	XD-VIOLENCE	UCF-CRIME
	$\mathcal{AP}^M$	$\mathcal{A}_M$
Transformer	81.56	87.25
Distance Transformer	84.24	88.01
RWKV	85.33	88.34
Distance RWKV	<b>87.48</b>	<b>89.63</b>

Table VI presents the ablation study on the time series module. As shown in Table VI, different time series methods exhibit significant performance differences across the two benchmark datasets. Using the Transformer model, the system achieves 81.56  $\mathcal{AP}^M$  value and 87.25  $\mathcal{A}_M$  value on XD-Violence and UCF-Crime, respectively. When incorporating the distance-aware mechanism, the performance of the Distance Transformer improves, reaching 84.24  $\mathcal{AP}^M$  value and 88.01  $\mathcal{A}_M$  value on the two datasets. In comparison, the RWKV method further enhances performance, achieving 85.33  $\mathcal{AP}^M$  value on XD-Violence and 88.34  $\mathcal{A}_M$  value on UCF-Crime. The combination of RWKV with the distance-aware mechanism (Distance RWKV) yields the best results. These results indicate that the distance-aware mechanism effectively enhances violence monitoring capabilities in time series modeling, while RWKV demonstrates significant advantages in capturing temporal dependencies.

TABLE VII

COMPUTATIONAL COMPLEXITY COMPARISON

Methods	Feature	Parameter	FLOPS
I3D [6]	I3D	28M	186.9G
C3D [22]	C3D	78M	386.2G
VadCLIP[18]	Clip	36.5M	82.3G
STPrompt [17]	Clip	31.5M	44.8G
<b>RuleVM (Ours)</b>	Clip	28.8M	36.5G

Table VII aims to present the parameter count (Parameter)

and computational complexity (FLOPS) of the proposed RuleVM, C3D, I3D, VadCLIP, and STPrompt on the XD-Violence dataset. The parameter count represents the number of weights in the model, which is used to measure the model’s complexity and storage requirements, while FLOPS indicates the computational load required for a single forward pass. As shown in Table VII, the proposed RuleVM uses a distance-based attention mechanism combined with an RWKV module, replacing the traditional embedding similarity calculation in Transformers. This lightweight design significantly reduces both the model’s parameter counts and the computational cost for each forward pass.

It is noteworthy that current edge computing devices, such as the NVIDIA Jetson Nano, impose restrictions on model parameters and computational load. More specifically, the model parameters are limited to 100M, and the computational load is capped at 100G FLOPS, while the Google Coral Edge TPU restricts model parameters to 32MB. The proposed RuleVM meets the operational requirements of both devices, making it more suitable for edge computing environments compared to other methods.

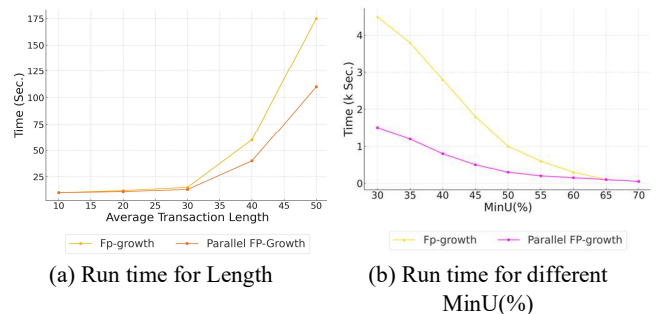


Fig.4. Ablation studies on Parallel FP-Growth

Figure 4 aims to present the ablation study of Parallel FP-Growth, consisting of two subplots that validate the feasibility of the proposed method from two perspectives. Subfigure (a) displays the execution times of the Fp-growth and Parallel FP-Growth methods across different transaction lengths. The x-axis represents the average transaction length, ranging from 10 to 50, while the y-axis represents the execution time in seconds (Sec.). As the average transaction length increases, both methods show an upward trend in execution time. However, the growth rate of Parallel FP-Growth is notably slower than that of Fp-Growth, indicating its higher efficiency.

Subfigure (b) shows the execution time comparison between Fp-Growth and Parallel FP-Growth under varying MinU(%) conditions. The x-axis represents the minimum usage threshold (MinU%) from 30% to 70%, and the y-axis represents the execution time in seconds (k Sec.). The graph illustrates that the execution time of both methods decreases with the MinU(%). However, Parallel FP-Growth consistently outperforms Fp-growth especially at lower MinU(%) values. These results indicate that Parallel FP-Growth is highly efficient, particularly at lower support thresholds, where it significantly reduces time.

Table VIII presents ablation studies on prompts in the XD-

Violence dataset. This experiment compares the proposed RuleVM with handcrafted prompts [33], learnable prompts [32], frame-level average prompts [18], and anomaly-specific prompts [17]. The results show that RuleVM achieves the best performance. The primary reason for RuleVM superior performance is that it leverages interpretable association rules mined directly from Yolo-World [20], combined with learnable parameters. This approach contrasts with other methods that rely on manually crafted labels or prompts generated by LLM, which may face issues such as limited interpretability, inconsistency, or overfitting to specific types of violence.

TABLE VIII

ABLATION STUDIES ON PROMPT

Prompt	AVG (%)
Hand-crafted Prompt	18.46 (-9.77)
Learnable-Prompt	23.84 (-4.39)
Average-Frame Visual Prompt	24.70 (-3.53)
Anomaly-Focus Visual Prompt	26.95 (-1.28)
<b>RuleVM (Ours)</b>	<b>28.23</b>



Fig. 5. Heat map visualization

Figure 5 illustrates the model interpretability visualized through heatmaps. It shows several violent scenes from the XD-Violence dataset, clearly demonstrating that the proposed RuleVM model not only identifies violent scenes but also precisely locates the areas of violence. This indicates that the RuleVM model has strong interpretability.

Figure 6 aims to illustrate the visualization of the proposed RuleVM system. As shown in the figure, when a video is input, the system can display the rules of the video content and generate output. Figure 6 presents four examples, showing that when the crowd size increases, the level of violence escalates from "fighting" to "rioting." To validate this finding, this study conducted a statistical analysis of videos in the "fights" and "riots" categories within the XD-Violence dataset. Specifically, the experiment used Yolo-World to monitor and count each frame in the videos and then output the top 10 most important objects. Figure 7 shows the proportion of each object in two different scenes. Fig. 7(a) represents the "Fight" scenario, where "Fist" has the highest proportion at 25%. Fig. 7(b) represents the "riot" scenario, where the two most prominent elements in the scene are "People" and "Person". This observation suggests that as crowd size increases during violent incidents, it is advisable to trigger quick alerts to prevent

escalation.

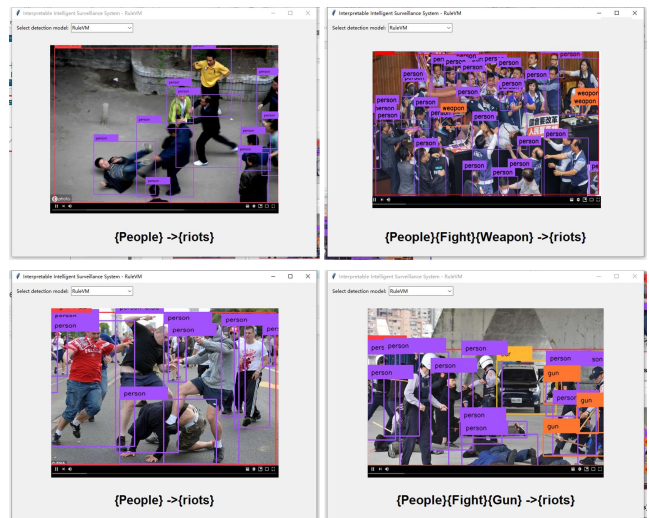
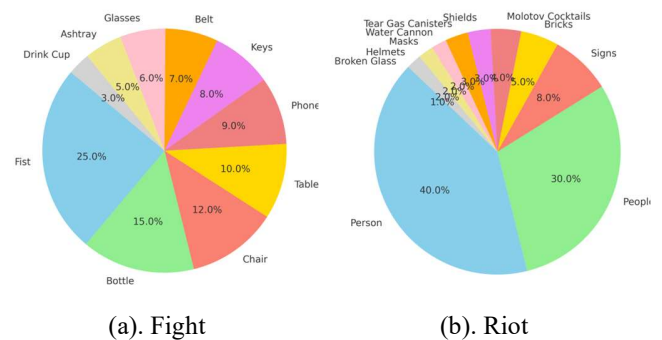


Fig. 6. The proposed RuleVM system visualization



(a). Fight

(b). Riot

Fig. 7. Top 10 important objects in Fight and Riot scene

## VI. CONCLUSION

This paper presents an interpretable RuleVM system for violence surveillance tasks. The system utilizes a dual branch structure to achieve accurate violence monitoring in both coarse-grained and fine-grained classifications, successfully integrating explicit and implicit knowledge representations, respectively, and significantly enhancing the system's interpretability.

In the implicit branch, the system uses only image features for coarse-grained binary classification, with image feature extraction divided into two channels: one responsible for scene frame extraction and the other focusing on action extraction. These are then combined and fed into a lightweight temporal attention module for sequence analysis, enabling effective feature extraction across different violent scenarios. In the explicit branch, the system performs fine-grained classification using language-image alignment. For text modality design, the system uses the YOLO-World model to monitor objects in video frames, identifying association rules through data mining methods as video descriptors. This dual-branch design provides RuleVM with strong interpretability in violence surveillance, balancing the requirements of coarse-grained and fine-grained monitoring.

Using XD-Violence and UCF-Crime as experimental datasets, results show that the proposed RuleVM significantly outperforms existing methods in terms of AP and AUC evaluation metrics. Additionally, the system reveals an interesting pattern: as crowd size increases, the level of violence also rises. This further demonstrates the system's powerful interpretability and its substantial potential for applications in areas such as intelligent surveillance and traffic monitoring.

## REFERENCES

- L. Ji, X. Liu, C. Zhang, S. Yang, and H. Li, "Fully Distributed Dynamic Event-Triggered Pinning Cluster Consensus Control for Heterogeneous Multiagent Systems With Cooperative-Competitive Interactions," *IEEE Trans. Syst., Man, Cybern.: Syst.*, vol. 53, no. 1, pp. 394-404, Jan. 2023.
- M. Wang, D. Zhou, and M. Chen, "Anomaly Monitoring of Nonstationary Processes With Continuous and Two-Valued Variables," *IEEE Trans. Syst., Man, Cybern.: Syst.*, vol. 53, no. 1, pp. 49-58, Jan. 2023.
- Z. Chen, K. Huang, D. Wu, C. Yang, and W. Gui, "Global Information-Based Lifelong Dictionary Learning for Multimode Process Monitoring," *IEEE Trans. Syst., Man, Cybern.: Syst.*, pp. 1-13, 2024, doi: 10.1109/TSMC.2024.3442168.
- P. Wu, X. Liu, and J. Liu, "Weakly Supervised Audio-Visual Violence Detection," *IEEE Trans. Multimedia*, vol. 25, pp. 1674-1685, 2023.
- J. He, Y. Ren, L. Zhai, and W. Liu, "FCC-MF: Monitoring Violence in Audio-Visual Context with Frame-Wise Cluster Contrast and Modality-Stage Flooding," *ICASSP 2024 - 2024 IEEE Int. Conf. Acoust., Speech Signal Process. (ICASSP)*, Seoul, Korea, Republic of, 2024, pp. 8346-8350.
- W. Sultani, C. Chen, and M. Shah, "Real-World Anomaly Detection in Surveillance Videos," in *Proc. IEEE Conf. Comput. Vis. Pattern Recognit. (CVPR)*, pp. 6479-6488, 2018.
- A. Dosovitskiy et al., "An image is worth 16x16 words: Transformers for image recognition at scale," *arXiv preprint arXiv:2010.11929*, 2020.
- A. Radford et al., "Learning transferable visual models from natural language supervision," in *Int. Conf. Mach. Learn. (ICML)*, PMLR, pp. 8748-8763, 2021.
- Y. Fan, Y. Yu, W. Lu, and Y. Han, "Weakly-Supervised Video Anomaly Detection With Snippet Anomalous Attention," *IEEE Trans. Circuits Syst. Video Technol.*, vol. 34, no. 7, pp. 5480-5492, July 2024.
- Q. Zhou, S. He, H. Liu, T. Chen, and J. Chen, "Pull & Push: Leveraging Differential Knowledge Distillation for Efficient Unsupervised Anomaly Detection and Localization," *IEEE Trans. Circuits Syst. Video Technol.*, vol. 33, no. 5, pp. 2176-2189, May 2023.
- C. Guo, H. Wang, Y. Xia, and G. Feng, "Learning Appearance-Motion Synergy via Memory-Guided Event Prediction for Video Anomaly Detection," *IEEE Trans. Circuits Syst. Video Technol.*, vol. 34, no. 3, pp. 1519-1531, March 2024.
- Q. Peng et al., "Coating Feature Analysis and Capacity Prediction for Digitalization of Battery Manufacturing: An Interpretable AI Solution," *IEEE Trans. Syst., Man, Cybern.: Syst.*, doi: 10.1109/TSMC.2024.
- R. Liu et al., "An Interpretable Multiplication-Convolution Network for Equipment Intelligent Edge Diagnosis," *IEEE Trans. Syst., Man, Cybern.: Syst.*, vol. 54, no. 6, pp. 3284-3295, June 2024.
- Z. Sun, W. Dong, J. Shi, and Z. Huang, "Interpretable Disease Progression Prediction Based on Reinforcement Reasoning Over a Knowledge Graph," *IEEE Trans. Syst., Man, Cybern.: Syst.*, vol. 54, no. 3, pp. 1948-1959, March 2024.
- T. Li et al., "WaveletKernelNet: An Interpretable Deep Neural Network for Industrial Intelligent Diagnosis," *IEEE Trans. Syst., Man, Cybern.: Syst.*, vol. 52, no. 4, pp. 2302-2312, April 2022.
- B. Zhang, Y. Dong, and W. Pedrycz, "Consensus Model Driven by Interpretable Rules in Large-Scale Group Decision Making With Optimal Allocation of Information Granularity," *IEEE Trans. Syst., Man, Cybern.: Syst.*, vol. 53, no. 2, pp. 1233-1245, Feb. 2023.
- P. Wu et al., "Weakly Supervised Video Anomaly Detection and Localization with Spatio-Temporal Prompts," in *Proc. ACM Multimedia*, 2024.
- P. Wu et al., "VadCLIP: Adapting Vision-Language Models for Weakly Supervised Video Anomaly Detection," in *Proc. AAAI Conf. Artif. Intell. (AAAI)*, 2024.
- C. Chang et al., "LLMScenario: Large Language Model Driven Scenario Generation," *IEEE Trans. Syst., Man, Cybern.: Syst.*, vol. 54, no. 11, pp. 6581-6594, Nov. 2024.
- T. Cheng et al., "YOLO-World: Real-Time Open-Vocabulary Object Detection," in *Proc. IEEE Conf. Comput. Vis. Pattern Recognit. (CVPR)*, 2024.
- P. Wu et al., "Not Only Look, but Also Listen: Learning Multimodal Violence Detection under Weak Supervision," in *Proc. Eur. Conf. Comput. Vis. (ECCV)*, pp. 322-339, 2020, Springer.
- M. Hasan et al., "Learning Temporal Regularity in Video Sequences," in *Proc. IEEE Conf. Comput. Vis. Pattern Recognit. (CVPR)*, pp. 733-742, 2016.
- Y. Ji and H. Lee, "Event-Based Anomaly Detection Using a One-Class SVM for a Hybrid Electric Vehicle," *IEEE Trans. Veh. Technol.*, vol. 71, no. 6, pp. 6032-6043, June 2022.
- J.-X. Zhong et al., "Graph Convolutional Label Noise Cleaner: Train a Plug-and-Play Action Classifier for Anomaly Detection," in *Proc. IEEE Conf. Comput. Vis. Pattern Recognit. (CVPR)*, pp. 1237-1246, 2019.
- Y. Tian et al., "Weakly-Supervised Video Anomaly Detection with Robust Temporal Feature Magnitude Learning," in *Proc. IEEE Int. Conf. Comput. Vis. (ICCV)*, pp. 4975-4986, 2021.
- X. Zhou et al., "Monitoring Twenty-Thousand Classes Using Image-Level Supervision," in *Proc. Eur. Conf. Comput. Vis. (ECCV)*, pp. 350-368, 2022, Springer.
- R. Mokady, A. Hertz, and A. Bermano, "ClipCap: CLIP Prefix for Image Captioning," *arXiv preprint arXiv:2111.09734*, 2021.
- K. Zhou et al., "Learning to Prompt for Vision-Language Models," *Int. J. Comput. Vis.*, vol. 130, no. 9, pp. 2337-2348, 2022.
- W. Yu et al., "Turning a CLIP Model into a Scene Text Detection," in *Proc. IEEE Int. Conf. Comput. Vis. (ICCV)*, pp. 4975-4986, 2023.
- Y. Rao et al., "DenseCLIP: Language-Guided Dense Prediction with Context-Aware Prompting," in *Proc. IEEE Conf. Comput. Vis. Pattern Recognit. (CVPR)*, pp. 18082-18091, 2022.
- H. Lv et al., "Unbiased Multiple Instance Learning for Weakly Supervised Video Anomaly Detection," in *Proc. IEEE/CVF Conf. Comput. Vis. Pattern Recognit. (CVPR)*, 2023.
- H. K. Joo et al., "Clip-tsa: CLIP-assisted Temporal Self-Attention for Weakly-Supervised Video Anomaly Detection," in *Proc. IEEE Int. Conf. Image Process. (ICIP)*, pp. 3230-3234, 2023.
- H. Luo et al., "CLIP4Clip: An Empirical Study of CLIP for End to End Video Clip Retrieval and Captioning," *Neurocomputing*, vol. 508, pp. 293-304, 2022.
- C. Wang, G. Sun, C. Wang, Z. Gao and H. Wang, "Monte Carlo-Based Restoration of Images Degraded by Atmospheric Turbulence," in *IEEE Trans. Syst., Man, Cybern.: Syst.*, vol. 54, no. 11, pp. 6610-6620, Nov. 2024.
- C. Xu et al., "Multiscale Neighborhood Adaptive Clustering Image Segmentation for Molten Iron Flow Slag-Iron Recognition," in *IEEE Trans. Syst., Man, Cybern.: Syst.*, vol. 54, no. 8, pp. 4642-4654, Aug. 2024.
- P. Bo et al., "RWKV: Reinventing RNNs for the Transformer Era," *arXiv preprint arXiv:2305.13048*, 2023.
- J. -F. Qu, P. Fournier-Viger, M. Liu, B. Hang and C. Hu, "Mining High Utility Itemsets Using Prefix Trees and Utility Vectors," in *IEEE Transactions on Knowledge and Data Engineering*, vol. 35, no. 10, pp. 10224-10236, 1 Oct. 2023.
- A. Banik and J. P. Singh, "Android Malware Detection by Correlated Real Permission Couples Using FP Growth Algorithm and Neural Networks," in *IEEE Access*, vol. 11, pp. 124996-125010, 2023.